Atmos. Chem. Phys. Discuss., 13, 29263–29301, 2013
www.atmos-chem-phys-discuss.net/13/29263/2013/
doi:10.5194/acpd-13-29263-2013

Atmospheric Chemistry and Physics
Discussions
Open Access

Variations of oxygen-18 in West Siberian precipitation during the last 50 yr

M. Butzin[1,2], M. Werner[1], V. Masson-Delmotte[3], C. Risi[4], C. Frankenberg[5], K. Gribanov[2], J. Jouzel[3], and V. I. Zakharov[2]

[1]Alfred Wegener Institute, Helmholtz Centre for Polar and Marine Research, Bremerhaven, Germany
[2]Climate and Environmental Physics Laboratory, Ural Federal University, Russia
[3]Institut Pierre Simon Laplace, Laboratoire des Sciences du Climat et de l'Environnement, France
[4]Laboratoire de Météorologie Dynamique, Jussieu, Paris, France
[5]Jet Propulsion Laboratory, California Institute of Technology, Pasadena, USA

Received: 1 October 2013 – Accepted: 28 October 2013 – Published: 8 November 2013

Correspondence to: M. Butzin (martin.butzin@awi.de)

Published by Copernicus Publications on behalf of the European Geosciences Union.

Abstract

Global warming is associated with large increase in surface air temperature and precipitation in Siberia. Here, we apply the isotope-enhanced atmospheric general circulation model ECHAM5-wiso to investigate the variability of δ^{18}O in West Siberian precipitation and the underlying mechanisms during the last fifty years, and to assess the potential of a recently opened monitoring station in Kourovka (57.04° N, 59.55° E) to successfully track large-scale water cycle and climate change in this area. Our model is constrained to atmospheric reanalysis fields to facilitate the comparison with precipitation δ^{18}O from observations. In Russia, annual-mean model surface temperatures agree within ±1.5 °C with climatological data, while the model tends to overestimate precipitation by 10–20 mm month^{-1}. Simulated precipitation δ^{18}O shows a southwest to northeast decreasing pattern. The simulated annual-mean and seasonal δ^{18}O results are in overall good agreement with observations from 15 Russian stations of the Global Network of Isotopes in Precipitation between 1970 and 2009. Annual-mean model results and measurements are highly correlated ($r^2 \sim 0.95$) with a root mean square deviation of ±1 ‰. The model reproduces the seasonal variability of δ^{18}O, which parallels the seasonal cycle of temperature, and the seasonal range from −25 ‰ in winter to −5 ‰ in summer. Analysing model results for the extended period 1960–2010, long-term increasing trends in temperature, precipitation and δ^{18}O are detected in western Siberia. During the last 50 yr, winter temperatures have increased by 1.8 °C. Annual-mean precipitation rates have increased by 2–6 mm month^{-1} 50 yr^{-1}. Long-term trends of precipitation δ^{18}O are also positive but at the detection limit (< 1 ‰ 50 yr^{-1}). Regional climate is characterized by strong interannual variability, which in winter is strongly related to the North Atlantic Oscillation. In ECHAM5-wiso, regional temperature is the predominant factor controlling δ^{18}O variations on interannual to decadal time scales with slopes of about 0.5 ‰ °C^{-1}. Focusing on Kourovka, the simulated evolution of temperature, δ^{18}O and, to a smaller extent, precipitation during the last fifty years is

synchronous with model results averaged over entire western Siberia, suggesting that this site will be representative to monitor future isotopic changes this region.

1 Introduction

For the last several decades, an unequivocal warming of the climate system has been reported, evident from observations of increasing global average air and ocean temperatures, widespread melting of snow and ice and rising global-mean sea level (IPCC, 2007). However, while the rate of global warming averaged over the last 50 yr amounts about 0.1 °C per decade, high latitudinal to Arctic regions of the Northern Hemisphere, such as Siberia, have been warming at considerably higher rates (e.g., Tingley and Huybers, 2013, and references therein). Among others, positive feedbacks associated with snow and sea-ice albedo, water vapour and clouds, greenhouse effect, and moisture transport, as well as complex land surface – atmosphere interactions have been discussed as the possible reason for the observed Arctic amplification (e.g. Screen and Simmonds, 2000; Polyakov et al., 2002; Holland and Bitz, 2003; Serreze and Francis, 2006; Bekryaev et al., 2010; Taylor et al., 2013). While most studies so far have been focussed on the observed present and predicted future temperature increase, it is so far less determined how much other components of the Arctic climate system like the hydrological cycle will also change as a consequence of the temperature rise. Bengtsson et al. (2011) have estimated that the strength of the Arctic water cycle, in terms of annual precipitation may, increase by some 25 % until the end of this century.

Since the pioneering work of Dansgaard (1953, 1964), Craig (1961), Merlivat et al. (1973), Sonntag et al. (1976), and others, it is well known that changes in climate and the atmospheric water cycle leave an imprint in the isotopic composition of different water reservoirs on Earth. For meteoric water, Dansgaard (1964) explained successfully through the atmospheric distillation process the linear relation between the isotopic composition of precipitation and the local temperature at the precipitation site (the so-called "temperature effect") observed in many mid- to high latitude regions on

ACPD
13, 29263–29301, 2013

Earth. Given the magnitude of Arctic warming over the past decades, climate change should be recorded in the isotopic composition of meteoric waters (or natural archives) in boreal regions of the Northern Hemisphere.

Unfortunately, isotope records of present-day boreal precipitation are sparse and discontinuous. For Russia, Kurita et al. (2004) have reviewed the modern isotope climatology. Data from 13 Russian monitoring sites sampled during the period 1996–2000 depict a negative zonal isotopic gradient over Russia, which is explained by the gradual rain-out of moist, oceanic air masses, which are transported towards and over Russia by westerly winds. This isotopic gradient is weaker in summer, due to continental moisture recycling. Altogether, Kurita et al. (2004) estimate that 55 % of the summertime isotopic variability in Russian precipitation are linked to temperature changes and variations of the recycling ratio of continental water sources, the latter effect accounting for about 20 % of the signal. Combining simulation results of the isotope-enabled atmospheric general circulation model (AGCM) LMDZiso with satellite-based estimates of the isotopic composition of water vapour, Risi et al. (2013) also found that variations in continental recycling are minor contributions to the variability of isotope variations in high latitude precipitation.

To study the impact of climate change in West Siberia, the Russian "mega-grant" research project "Impact of climate change on water and carbon cycles of western Siberia" (WSibIso, http://wsibiso.ru) has recently started monitoring the isotopic composition of water vapour and precipitation at two high-latitude sites in western Siberia. At Kourovka Observatory (57.04° N, 59.55° E), located approx. 80 km west of Yekaterinburg, isotope monitoring has started in 2012 (Gribanov et al., 2013), while regular isotope measurements at Labytnangi (66.65° N, 66.40° E) have started in summer 2013.

Within the WSibIso Project, the understanding of the signals recorded at Kourovka and Labytnangi is supported by state-of-the-art climate simulations with two AGCMs equipped with explicit stable water isotope diagnostics, ECHAM5-wiso (Werner et al., 2011) and LMDZiso (Risi et al., 2010a). Such isotope-enabled AGCMs provide a mech-

Discussion Paper | Discussion Paper | Discussion Paper | Discussion Paper |

ACPD

13, 29263–29301, 2013

Variations of oxygen-18 in west Siberian precipitation

M. Butzin et al.

anistic understanding of the atmospheric processes influencing the isotopic composition of meteoric water. Since the pionneering work of Joussaume et al. (1984), Jouzel et al. (1987), Hoffmann et al. (1998) and others, about a dozen different state-of-the-art GCMs have been equipped with explicit isotope diagnostics (see Sturm et al., 2010, for a detailed model overview). A number of studies have clearly demonstrated their usefulness for an improved climatic interpretation of present and past water isotope variability (e.g., Jouzel et al., 2000; Mathieu et al., 2002; Noone and Simmonds, 2002; Werner and Heimann, 2002; Vuille and Werner, 2005; Lee and Fung, 2008; Tindall et al., 2009; Risi et al., 2010b). A comparison of different models allows to evaluate the robust features, and to scrutinize each model's parameterizations.

For Kourovka Observatory, the observed variations of the surface vapour isotopic composition are very similar to the results of the ECHAM5-wiso simulation covering the period April to September 2012 (Gribanov et al., 2013). Both exhibit short-term fluctuations on time scales from a few hours to a few days. These variations can be attributed to the passage of synoptic-scale weather systems, advecting air from different source regions with different isotopic signatures to Kourovka (Gribanov et al., 2013). A detailed comparison of the Kourovka data with LMDZiso model results will be presented in an accompanying paper (Gryazin et al., 2013).

Here, we evaluate the performance of ECHAM5-wiso (Werner et al., 2011) in West Siberia through a systematic comparison between simulated and observed precipitation δ^{18}O for the last decades. This analysis is based on a so-called "nudged" climate simulation performed for 1957–2013, covering the entire period of available ECMWF reanalysis data (Uppala et al., 2005; Berrisford et al., 2009; Dee et al., 2011). The model results are confronted to precipitation δ^{18}O data from 15 Russian stations being part of the Global Network of Isotopes in Precipitation (GNIP; IAEA/WMO, 2013). The analyses presented in this study focus on three key questions: (a) How well does the ECHAM5-wiso model capture the mean spatial and seasonal patterns of precipitation δ^{18}O in western Siberia? (b) How much has the isotopic composition of precipitation varied in western Siberia over the last five decades and what are the main mechanisms

ACPD
13, 29263–29301, 2013

and processes causing the variations? (c) How well can large-scale West Siberian climate and water cycle variations be observed in the isotopic composition of precipitation at Kourovka Observatory, one of the key monitoring sites within the WSibIso project?

2 Methods

2.1 Model description

Atmospheric simulations were carried out using ECHAM5-wiso (Werner et al., 2011), which is the isotope-enhanced version of the atmospheric general circulation model ECHAM5 (Roeckner et al., 2003, 2006; Hagemann et al., 2006). The model considers both stable water isotopes $H_2{}^{18}O$ and HDO, which have been explicitly implemented into its hydrological cycle, analogous to the isotope modelling approach used in the previous model versions ECHAM3 (Hoffmann et al., 1998) and ECHAM4 (e.g. Werner et al., 2001). For each phase of "normal" water (vapour, cloud liquid, cloud ice) being transported independently in ECHAM5, a corresponding isotopic counterpart is implemented in the model code. Isotopes and "normal" water are described identically in the AGCM as long as no phase transitions are concerned. Therefore, the transport scheme both for active tracers (moisture, cloud liquid water) and for the corresponding passive tracers (moisture, cloud water and cloud ice of the isotopes) is the flux-form semi-Lagrangian transport scheme for positive definite variables implemented in ECHAM5 (Lin and Rood, 1996).

Additional fractionation processes are defined for the water isotope variables whenever a phase change of the "normal" water occurs in ECHAM5, considering equilibrium and non-equilibrium fractionation processes. Equilibrium fractionation takes place if the corresponding phase change is slow enough to allow full isotopic equilibrium (Merlivat and Jouzel, 1979). On the other hand, non-equilibrium processes depend even on the velocity of the phase change, and therefore on the molecular diffusivity of the water isotopes (Jouzel and Merlivat, 1984). Processes involving isotopic fractionation include

ACPD
13, 29263–29301, 2013

the evaporation from the ocean, condensation either to liquid or to ice, as well as re-evaporation of liquid precipitation within the atmosphere. For evapotranspiration from land surfaces, possible isotopic fractionation is neglected (see Hoffmann et al., 1998, and Haese et al., 2013, for a detailed discussion of this issue).

ECHAM5-wiso has been evaluated against observations of isotope concentrations in precipitation and water vapour, both on a global as well as on a European scale (Langebroek et al., 2011; Werner et al., 2011). On both scales, annual and seasonal ECHAM-5-wiso simulation results are in good agreement with available observations from the Global Network of Isotopes in Precipitation, GNIP (IAEA-WMO, 2013).

Werner et al. (2011) have shown that the simulation of water isotopes in precipitation clearly improves with increased horizontal and vertical model resolution. Thus, for this study, we choose a horizontal model resolution of T63 in spectral space (horizontal grid size of approx. $1.9^\circ \times 1.9^\circ$), and a vertical resolution of 31 levels on hybrid sigma-pressure coordinates. Local ECHAM5-wiso results for GNIP stations (discussed further below) were obtained by bilinear interpolation to the station coordinates. To ensure a most realistic simulation of present-day climate variability, the model is forced with prescribed yearly values of present-day insolation and greenhouse gas concentrations (IPCC, 2000), as well as with monthly varying fields of sea-surface temperatures and sea-ice concentrations according to ERA-40 and ERA-Interim reanalysis data (Uppala et al., 2005; Berrisford et al., 2009; Dee et al., 2011). Furthermore, the dynamic-thermodynamic state of the ECHAM model is constrained to reanalysis data by an implicit nudging technique (Krishamurti et al., 1991; the implementation in ECHAM is described by Rast et al., 2013), i.e. modelled fields of surface pressure, temperature, divergence and vorticity are relaxed to the corresponding ERA-40 and ERA-Interim reanalysis fields (Uppala et al., 2005; Berrisford et al., 2009; Dee et al., 2011). The nudging interval is 6 h, ensuring that the simulated large-scale atmospheric flow is modelled in agreement with the ECWMF reanalysis data on all analysed time scales. In contrast to the atmospheric flow, the hydrological cycle and its isotopic variations is still fully prognostic and not nudged to any reanalysis data.

ACPD
13, 29263–29301, 2013

The performed simulation covers the period 1 September 1957 until July 2013. Here we regard the first 28 months as model spin-up and analyse in this study the 51 yr period between 1960 and 2010. If not stated otherwise, we focus on monthly averaged model results of the isotopic composition of precipitation (typically expressed in a delta-notation as δ^{18}O or δD), covering the full period of available stable water isotope measurements in Russia.

2.2 Observations of isotopes in Russian precipitation

In western Siberia (here defined as the region ranging from 55° E–90° E and 55° N–70° N), monthly precipitation δ^{18}O data are available from 9 GNIP stations operating for different time periods between 1973 and 2000. Individual records range from a few months to up to ten years. Given the sparseness of these observations, we also include in this study data from 12 other GNIP stations in Russia for an improved model evaluation.

To this set of 21 GNIP stations, we applied the following data selection: (a) We considered only stations where the sampling period of isotopes in precipitation was at least five years; (b) Unrealistic delta values of approx. +50 ‰ for both HDO and $H_2^{18}O$ isotopes from Amderma are excluded; (c) Five outliers with anomalous positive delta values from Barabinsk and Yaktutsk stations are excluded; (d) Stations where reported monthly mean temperatures disagree by more than 10 °C from WMO measurements and/or ECWMF reanalysis values (indicating problems with data quality control within the GNIP database) are excluded. This issue concerns Kandalaksa, Khanty-Mansiysk, Kursk, Olenek, Salekhard, and Terney.

After data filtering, our database consists in results from 15 GNIP stations (comprising 1161 monthly observations of δ^{18}O between 1970 and 2009; Table 1) used hereafter for further analyses.

ACPD
13, 29263–29301, 2013

2.3 Satellite observations of isotopes in water vapour

Although precipitation and water vapour have a different isotopic composition due to fractionation processes, a comparison of ECHAM5-wiso results for isotopes in water vapour with available data from satellite and ground-based remote sensing techniques is valuable. It will reveal some first-order information if the model simulates the spatial gradients of the isotopic signal in atmospheric water vapour (and thus consequently also in precipitation) over Russia in a correct manner. Ground-based remote sensing of δ^{18}O in water vapour has been realized recently (Rokotyan et al., 2013) but so far, only few point measurements have been carried out. For this reason we consider global observations of deuterium (δD) in total column water vapour retrieved from the GOSAT satellite (Boesch et al., 2013; Frankenberg et al., 2013) for the period April 2009 to June 2011. The data were first shown by Risi et al. (2013) who also present a thorough description of data quality criteria, spatiotemporal sampling issues and convolution procedures. Following Risi et al. (2013), ECHAM5-wiso results have been convolved with averaging kernels for a rigid comparison with GOSAT retrievals.

3 Results and discussion

3.1 Present-day mean climate

Gribanov et al. (2013) showed that the ECHAM5-wiso simulation results agree well with observations from Kourovka Observatory and the surrounding area. Surface temperatures and precipitation rates in Yekaterinburg (WMO data for station Sverdlovsk retrieved from the KNMI Climate Explorer, http://climexp.knmi.nl) were compared to the ECHAM5-wiso model values (calculated as the mean over the period 1960–2010). Simulated mean monthly surface temperatures show a small cold bias of less than 1 °C in the annual mean, with larger deviations (of up to −3 °C) in winter. Precipitation rates simulated by ECHAM are slightly above observed values in winter (by 5–

10 mm month^{-1} between November and March), but up to −18 mm month^{-1} lower between July and September.

Figure 1 shows annual-mean patterns of simulated surface temperature (T), total precipitation amount (P), and oxygen-18 content of precipitation (δ^{18}O) for the region 0–160° E, 40–80° N, covering central and eastern Europe, Russia and parts of Asia.

Surface temperatures (Fig. 1a) decrease from southwest to northeast. Comparing model temperatures averaged over 1960–2010 with the CRU temperature reconstruction for the same period (University of East Anglia Climatic Research Unit (CRU), Jones and Harris, 2013), we find slightly colder values in the simulations than observed (in the range from −0.5 to −1.5 °C) in Eurasia and western Siberia. Conversely, simulated temperatures in Central and eastern Siberia are higher by ~ 0.5–1.5 °C than the CRU data, with maximum differences of up to 5 °C found for the Verkhoyansk Range.

Precipitation fields (Fig. 1b) are zonally aligned in the simulated annual mean pattern. Total precipitation decreases from 60–80 mm month^{-1} at the East European Plain eastwards and arrives at minimum values of 20–30 mm month^{-1} in a zone ranging from the southern part of the West Siberian Plain to Northeast Siberia. Precipitation values peak in the Russian Far East in the Stanovoy Range. Compared to the CRU precipitation reconstruction (University of East Anglia Climatic Research Unit (CRU), Jones and Harris, 2013), simulated precipitation is higher by 10–20 mm month^{-1} north of 60° N, and by up to about 30 mm month^{-1} in the Russian Far East mountain areas. In the southern part of the West Siberian Plain ECHAM produces slightly less precipitation than observed. The precipitation deficit becomes stronger with increasing continentality.

The simulated annual mean δ^{18}O values of precipitation over Russia are plotted in Fig. 1c. Within Russia, δ^{18}O values decrease from southwest to northeast. In contrast to temperature and precipitation, no global dataset of observed δ^{18}O in precipitation exists for comparison, yet. The location of the available Russian GNIP stations, also plotted in Fig. 1c, clearly demonstrates the sparseness and existing lack of information for observed present-day values of δ^{18}O in precipitation over Russia.

Total column water vapour values of δD according to ECHAM5-wiso and to GOSAT satellite retrievals are shown in Fig. 2. As there is no absolute calibration for column-integrated δD of GOSAT (Risi et al., 2013) we focus on the spatial distribution. The model captures the pattern of total column water vapour δD variations over Russia well (Fig. 2a and b). Even some details such as a patch of depleted δD values southwest of Kourovka Observatory are resolved. Regarding the meridional δD gradient along the longitude zone including Kourovka, ECHAM5-wiso captures the northward depletion retrieved by GOSAT (Fig. 2c). Considering the zonal δD variation along the latitude zone including Kourovka (Fig. 2d), we find that ECHAM5-wiso tends to underestimate the eastward depletion associated with the continental effect.

For more quantitative analyses, we compare the climatology from our ECHAM5-wiso simulation results to available GNIP measurements. For each GNIP location, we restrict the data-model comparison to those months within period 1960–2010, when measurements have been reported (see Table 1 for details). Thus, mean values of T, P and δ^{18}O are calculated over different periods for each GNIP station and from ECHAM5-wiso.

As expected from our nudging strategy, Fig. 3a shows a good agreement between modelled surface temperatures and GNIP observations which are highly correlated ($r^2 \sim 0.95$). The root mean square (RMS) difference between model results and observations is ±1.1 °C. A linear fit indicates that ECHAM5-wiso tends to underestimate the observed temperatures by 0.6 °C. The largest difference is found for Perm, where the model is too cold by 2.9 °C. For precipitation the scatter of model results is larger (Fig. 3b). The RMS difference between simulations and observations is about ±10 mm month^{-1}, with the largest deviations for Murmansk (+24 mm month^{-1}) and for Rostov (−19 mm month^{-1}). The linear regression between simulations and observations points to a moist bias of ECHAM5-wiso by about 7 mm month^{-1}. Figure 3c indicates that ECHAM5-wiso captures annual mean δ^{18}O records in Russia reasonably well. Model results and GNIP data are highly correlated ($r^2 \sim 0.95$), and the RMS difference amounts ±1 ‰. Maximum differences of up to +4 ‰ are found for

ACPD
13, 29263–29301, 2013

Title Page
Abstract | Introduction
Conclusions | References
Tables | Figures
◀| |▶
◀ ▶
Back | Close
Full Screen / Esc
Printer-friendly Version
Interactive Discussion

two stations in eastern Siberia (Cherskiy and Yakutsk) where ECHAM5-wiso does not simulate sufficient depletion. The linear relationship between simulated and observed δ^{18}O data yields a slope of 0.85. The model-data deviations are mainly dominated by a misfit of ECHAM5-wiso values with eastern Siberian GNIP observations. The reason for this disagreement deserves further investigations, as there is no corresponding flaw of simulated surface temperatures and precipitation values at these locations. The model slightly underestimates the spatial gradients of δ^{18}O observed in Russia. The meridional isotope gradient (observed slope: −4.2 ‰ $10^{\circ -1}$ latitude, simulated slope: −3.6 ‰ $10^{\circ -1}$ latitude), reflecting the meridional temperature gradient, is by about a factor of four to five larger than the zonal isotope variation (observed slope: −0.9 ‰ $10^{\circ -1}$ longitude, simulated slope: −0.8 ‰ $10^{\circ -1}$ longitude) associated with increasing continentality (not shown).

Studying anomalies of δ^{18}O ($\Delta\delta^{18}$O) and surface temperatures (ΔT), we find a linear relationship for all seasons with a typical slope of 0.5 ‰ °C^{-1} (Fig. 4). The correlation between GNIP ΔT and $\Delta\delta^{18}$O is most pronounced in autumn (SON, $r^2 = 0.69$) and winter (DJF, $r^2 = 0.61$). In spring (MAM, $r^2 = 0.50$) and summer (JJA, $r^2 = 0.40$) the correlation is weaker, but still significant ($p \ll 0.05$ applying a t test). The weaker coupling indicates that the δ^{18}O signal during the warm season is significantly affected by other processes such as moisture recycling. ECHAM5-wiso simulates a similar seasonal relationship but the correlation between $\Delta\delta^{18}$O and ΔT is higher than for the observations ($r^2 = 0.50$–0.79). The model overestimates the coupling between $\Delta\delta^{18}$O and ΔT especially in spring ($r^2 = 0.79$).

We now compare the simulated and observed seasonal cycle of precipitation δ^{18}O in western Siberia (Fig. 5). The data exhibit seasonal variations ranging from −25 ‰ to −5 ‰ with minimum values in winter and maximum values in summer, closely following the seasonal cycle of temperature. Peak values of up to −1 ‰ were observed in Perm during the second half of the 1980s. Despite the reported small annual-mean temperature biases, ECHAM5-wiso correctly simulates the timing and magnitude of the seasonal variations of both temperature and δ^{18}O (Fig. 5) in western Siberia. Observa-

ACPD
13, 29263–29301, 2013

tions and simulations from Pechora and Perm also show inter-annual variations, which will be discussed in the next section.

3.2 Interannual to decadal variations over the last five decades

The sampling period of precipitation δ^{18}O in Russia is too short for a thorough investigation of the long-term variability seen in recent west Siberian isotope and climate records. To overcome this problem, we extend the time frame by considering model results for the period 1960–2010. Therefore, the following analysis of interannual to decadal variations of T, P and δ^{18}O over Russia during the last decades is entirely based on model outcomes. If not stated otherwise, the model results are presented as anomalies from their long-term climatological mean (1961–1990). A zero-phase bidirectional low-pass filter with a length of 24 equally weighted months is employed on the ECHAM5-wiso results to highlight long-term variability.

At the global scale, (Fig. 6a, blue line), surface warming has been accompanied by increasing atmospheric moisture (not shown) while modelled precipitation over land has stayed constant or maybe even slightly decreased (Fig. 6b). In parallel, global water vapour and precipitation have become progressively enriched with heavy water isotopes (Fig. 6c). A linear regression analysis indicates a long-term increase of global land surface temperatures by 0.7 °C 50 yr^{-1} in the annual mean which is in the range of reconstructions (for a compilation see Trenberth et al., 2007, and references therein). Simulated anomalies of global land precipitation peaked in the mid-1970s and decreased until the late 1980s, recovering to positive values until 2000. The negative precipitation trend until 1990 is qualitatively in line with reconstructions but the simulated recovery until 2000 is smaller than observed (Trenberth et al., 2007; note that precipitation trends there relate to the different period 1981–2000).

Long-term trends in T, P, and δ^{18}O are also found in western Siberia (averaged over the area 55° E–90° E, 55° N–70° N) as well as at Kourovka site (Fig. 6, red and green lines). Regional and local warming occurred at higher rates (1.2 °C 50 yr^{-1} averaged over western Siberia and 1.0 °C 50 yr^{-1} in Kourovka in the annual mean). The

ACPD
13, 29263–29301, 2013

long-term warming is particularly pronounced in the winter season (DJF), especially in western Siberia and Kourovka, where DJF warming rates are 1.8 °C 50 yr^{-1}. Our model also exhibits a positive long-term trend of precipitation. For both western Siberia and Kourovka, annual-mean precipitations rates have been increasing by 2–6 mm $month^{-1}$ during the last 50 yr, with a tendency towards enhanced DJF precipitation at the expense of JJA rainfall. Long-term trends of precipitation $\delta^{18}O$ are also positive but the changes are small and at the detection limit (< 1 ‰ 50 yr^{-1}). For western Siberia and Kourovka we find that the long-term changes of $\delta^{18}O$ are more pronounced during JJA than during DJF, which is opposite to the simulated seasonal temperature trends. The reason for this decoupling is that we simulate increasing moisture import to western Siberia in summer while this is not the case in winter (not shown). As a consequence, the isotopic signature of moisture available for precipitation is less affected by continental depletion during recent summer seasons than during recent winters.

At the regional and local scale the long-term trends are superimposed by strong interannual variability reaching values of up to ±1.5 °C, ±10 mm yr^{-1}, and ±1 ‰, respectively. Temperature anomalies simulated for western Siberia and Kourovka covary since the late 1960s. During most of the simulation period, temperature differences between western Siberia and Kourovka are less than about ±0.5 °C, with Kourovka showing larger fluctuations than western Siberia. Simulated precipitation anomalies for western Siberia and Kourovka appear to be less synchronous than it is the case for temperature, in particular between 1995 and 2000 when the precipitation curves are out of phase. Moreover, in Kourovka the precipitation variability is considerably larger (by up to 10 mm $month^{-1}$) than its average for western Siberia. The larger deviation between the mean precipitation amount in West Siberia and the values in Kourovka as compared to the surface temperatures is not surprising, as precipitation is known to strongly vary at short spatial and temporal length scales. Consistent with the temperature patterns, anomalies of $\delta^{18}O$ in western Siberia and Kourovka are most of the time in phase and differ within ±0.5 ‰ with the larger variability being simulated for Kourovka. In our simulation, $\delta^{18}O$ and surface temperature mostly covary, which is

ACPD
13, 29263–29301, 2013

not the case for precipitation amount. However, δ^{18}O and temperature are not coupled in a rigid manner. This is indicated by our model results for the years around 1990, when temperatures in Kourovka were below the western Siberian average while the opposite is obtained for δ^{18}O. The overall good agreement between mean temperature and δ^{18}O changes in West Siberia and Kourovka is a key finding with respect to the objectives of the WSibIso Project. It indicates that Kourovka Observatory is a well-representative site to monitor climate change in western Siberia.

While we find that annual and seasonal-mean values of T, P and δ^{18}O have been slowly increasing during the last decades, we do not arrive at a clear tendency regarding their interannual variance. Compared with the interannual variance between 1961 and 1990 (estimated from the standard deviation of detrended model results), the last decade (2001–2010) is characterized by increased variability of winter temperatures (0.4 °C) and winter precipitation (2 mm month^{-1}) in western Siberia, and by increased variance of winter and summer precipitation rates (3 mm month^{-1}) in Kourovka. The last decade does not exhibit substantial changes in δ^{18}O variability.

Further analyses of the temporal correlation between simulated values δ^{18}O in precipitation and surface temperatures (Fig. 7) reveal that the correlation of annual-mean values seen in Fig. 7a is mainly controlled by a strong linkage between surface temperature and δ^{18}O in precipitation in western Siberia during winter (DJF). While the correlation coefficient between winter T and δ^{18}O can reach maximum values of up to 0.9 (Fig. 7b), the correlation between both climate variables is substantially weaker for summer (Fig. 7c). In the WSibIso target area, only one quarter of the observed interannual δ^{18}O variability can be explained by a linear relationship with local surface air temperature changes.

We now explore the relationship between West Siberian climate and precipitation isotopic composition, and large-scale atmospheric circulation. Previous studies have revealed a strong linkage between surface temperatures, δ^{18}O in precipitation and the North Atlantic Oscillation (NAO) for major parts of Europe (e.g., Baldini et al., 2008; Field, 2010; Langebroek et al., 2011; Casado, et al., 2013). It is also known that the

ACPD
13, 29263–29301, 2013

influence of the NAO on the large-scale atmospheric circulation is not bound to Europe but extends further east towards Russia (e.g. Halpert and Bell, 1997). Correlating simulated δ^{18}O values in Kourovka with the simulated global sea level pressure field, we find for the winter season a pattern which is characteristic for the NAO (Fig. 8; cf. Hurrell and Deser, 2009). Thus, as a next step we investigate the influence of NAO variations on temperature and δ^{18}O variability over Russia.

Figure 9 shows the observed and simulated station-based NAO seasonal winter (DJF) index for the period 1960–2010. ECHAM5-wiso model faithfully captures the observed NAO index (Hurrell et al., 2013) consistent with the reanalysis pressure fields used for nudging. Minor deviations between the observed station-based index and the modelled values can be attributed to the chosen model resolution T63, which can result in a slightly different average surface pressure of a relatively large grid box as compared to a point-like station location. A correlation analyses of this simulated station-based NAO seasonal winter (DJF) index with modelled values of T, P, and δ^{18}O reveals that the NAO influence on surface temperature, precipitation amount and δ^{18}O in precipitation extends in a broad band from Europe until Northern Siberia (Fig. 10). To a large extent, the covariation between winter NAO and δ^{18}O (Fig. 10a) is controlled by air temperature. Winters are mild in years when the NAO is strong, which is indicated by the positive correlation between NAO index and DJF surface temperatures shown in Fig. 10b. Winter precipitation in Northern Russia also increases when the NAO is strong (Fig. 10c). Further analyses reveal that the correlation between NAO and winter precipitation is also associated with enhanced moisture transport from the subtropical North Atlantic, implying a shift of the moisture source regions (Fig. 11a). Conversely, when the NAO is weak, the origin of atmospheric moisture import shifts towards the Arctic Ocean (Fig. 11b).

In a recent modelling study assessing the effect of precipitation intermittency on the temporal correlation between seasonal temperatures and the NAO, Casado et al. (2013) found that precipitation weighting of temperatures reduces the correlation strength in eastern Siberia during the winter season. While our results are based on unweighted monthly temperatures, we additionally assessed the effect of precipitation weighting for the winter season. We find that the correlation decreases in Northern Siberia (not shown) which partly supports the findings by Casado et al. (2013). However, the effect is probably overestimated as our calculation employs monthly values, while Casado et al. (2013) showed that precipitation weighting should be carried out for daily or even shorter time intervals. Regarding the results for unweighted temperatures as well as for $\delta^{18}O$ which Casado et al. (2013) obtained using the LMDZiso model, LMDZiso shows a weaker response to the winter NAO than ECHAM5-wiso. This is probably due to the different nudging strategies, as the LMDZiso model is only nudged to the wind field while ECHAM5-wiso is also nudged to temperatures.

Our analyses show that in wintertime the influence of NAO-associated atmospheric circulation changes have a slightly weaker impact on precipitation $\delta^{18}O$ over west Siberia than on the surface temperatures in this region. On the contrary, $\delta^{18}O$ in precipitation is much more strongly correlated to the NAO than the precipitation amount itself. Previous studies have argued that variations of $\delta^{18}O$ in precipitation are rather a regionally integrated signal of several climate variables than a proxy for either local temperature or precipitation changes (e.g., on a global scale: Schmidt et al., 2005; for western Europe: Langebroek et al., 2011). Our findings only partly agree with these studies and rather reveal that both $\delta^{18}O$ and local temperatures in western Siberia are influenced by NAO variations in a similar matter. Our results also expose the potential of reconstructing past changes of the NAO strength from various $\delta^{18}O$ records, e.g. retrieved from lake sediments, speleothems, or tree-rings (e.g., Sidorova et al., 2010) from this region. However, the ECHAM5-wiso results indicate that archives storing the $\delta^{18}O$ signal of winter precipitation should be suitable for such a NAO reconstruction.

While the interannual variability of $\delta^{18}O$ in winter precipitation can be largely attributed to temperature variations in western Siberia associated with the NAO, we do not find such a teleconnection for the summer season. Previous studies have shown that evapotranspiration fluxes significantly contribute to summer precipitation in Russia, and estimated that the regional moisture recycling rates can exceed 80 % (e.g.,

ACPD
13, 29263–29301, 2013

Koster et al., 1993; Numaguti, 1999; Risi et al., 2013). Accordingly, Kurita et al. (2003, 2004) have suggested that snow melt and subsequent evaporation of soil moisture carrying the isotopic imprint of winter precipitation could significantly influence the isotopic composition of regional precipitation, counterbalancing the positive coupling between temperature and δ^{18}O. Our model results partly support this hypothesis. We find that the summertime δ^{18}O signal is correlated with sea level pressure only above the western Siberian Plain, which is associated with a shift of atmospheric moisture fluxes from predominantly western to northwestern source regions (Fig. 12). In those regions, precipitation δ^{18}O is negatively correlated with soil wetness and evaporation fluxes, but positively correlated with the isotopic composition of the soil water pool and the evaporate (not shown). However, the correlation between δ^{18}O and evaporation is weak. This may be due to the fact that we considered monthly averages, while the atmospheric lifetime of evaporated water vapour is a few days. Thus, our results are probably overly smoothed to fully resolve the imprint of moisture recycling on δ^{18}O. We also observe a greater variability of atmospheric moisture transport towards Kourovka during the summer season than during the winter season. JJA fluxes vary within $\sim \pm 35\,\%$ in magnitude and within $\sim \pm 25^{\circ}$ in flow direction, while DJF fluxes vary within $\sim \pm 10\,\%$ in magnitude and $\sim \pm 15^{\circ}$ in flow direction, respectively. The weak link between δ^{18}O and local climate during the summer season deserves further investigations (using for instance water tagging methods) beyond the scope of this study.

4 Summary and conclusions

Using the few available observations as well as a new simulation from the isotope-enhanced atmospheric general circulation model ECHAM5-wiso covering the period 1958–2013, we have investigated the spatiotemporal variations in the isotopic composition of precipitation in Russia during the last decades. In its nudged configuration, the model simulates temperature and precipitation fields over western Siberia within reasonable error margins, providing a realistic framework to investigate the model performance for $\delta^{18}O$. The model reproduces the spatial pattern of precipitation $\delta^{18}O$ when compared with averaged observations from 15 stations of the Global Network of Isotopes in Precipitation between 1970 and 2009. The model fails to capture the amount of $\delta^{18}O$ depletion in eastern Siberia while temperature and precipitation are correctly simulated.

According to our model results, temperature is the predominant factor controlling the variability of annual-mean and winter precipitation $\delta^{18}O$ in Russia on interannual to decadal time scales. Interannual variations in winter temperature and isotope signals show a strong imprint of the North Atlantic Oscillation. During the summer season, local temperature has only a minor impact on the isotopic composition of precipitation. Our analyses support the importance of moisture recycling, involving the delayed reevaporation of isotopically depleted winter precipitation retained in snow melt and soil water. We also find enhanced variability of moisture transport and hence source regions during the summer season. The relative importance of these two processes should be further investigated using second order isotopic data (e.g. d-excess) as well as moisture tagging diagnostics.

Recent observations reveal significant isotopic variability on the diurnal and daily time scale (Gribanov et al., 2013). The impact of short-term variations on the isotopic signal seen in the monthly GNIP records cannot be analysed, but continuous monitoring of water vapour $\delta^{18}O$ and daily sampling of precipitation $\delta^{18}O$ will permit to study processes at the event scale. Regarding Kourovka Observatory, where such a monitoring programme has recently been established, we find that the simulated variability of temperature and $\delta^{18}O$ at this location is similar to model results averaged over the entire West Siberian region. Therefore, we conclude that that this location is highly suitable to monitor isotopic changes all over in western Siberia.

Acknowledgements. This research was supported by a grant of the Russian government under the contract 11.G34.31.0064. The help of S. Rast, Max Planck Institute for Meteorology, Hamburg, for providing model support regarding ECHAM5 nudging aspects is thankfully acknowledged.

References

Baldini, L. M., McDermott, F., Foley, A. M., Baldini, J. U. L.: Spatial variability in the European winter precipitation $\delta^{18}O$–NAO relationship: implications for reconstructing NAO-mode climate variability in the Holocene, Geophys. Res. Lett., 35, L04709, doi:10.1029/2007GL032027, 2008.

Bekryaev, R. V., Polyakov, I. V., and Alexeev, V. A.: Role of polar amplification in long-term surface air temperature variations and modern arctic warming, J. Climate, 23, 3888–3906, doi:10.1175/2010JCLI3297.1, 2010.

Bengtsson, L., Hodges, K. I., Koumoutsaris, S., Zahn, M., and Keenlyside, N.: The changing atmospheric water cycle in Polar Regions in a warmer climate, Tellus A, 63, 907–920, 2011.

Berrisford, P., Dee, D., Fielding, K., Fuentes, M., Kallberg, P., Kobayashi, S., and Uppala, S.: The ERA-Interim archive, ERA Report Series, August 2009.

Boesch, H., Deutscher, N. M., Warneke, T., Byckling, K., Cogan, A. J., Griffith, D. W. T., Notholt, J., Parker, R. J., and Wang, Z.: HDO/H_2O ratio retrievals from GOSAT, Atmos. Meas. Tech., 6, 599–612, doi:10.5194/amt-6-599-2013, 2013.

Casado, M., Ortega, P., Masson-Delmotte, V., Risi, C., Swingedouw, D., Daux, V., Genty, D., Maignan, F., Solomina, O., Vinther, B., Viovy, N., and Yiou, P.: Impact of precipitation intermittency on NAO-temperature signals in proxy records, Clim. Past, 9, 871–886, doi:10.5194/cp-9-871-2013, 2013.

Craig, H.: Isotopic variations in meteoric waters, Science, 133, 1702–1703, 1961.

Dansgaard, W.: The abundance of ^{18}O in atmospheric water and water vapour, Tellus, 5, 461–469, 1953.

Dansgaard, W.: Stable isotopes in precipitation, Tellus, 16, 436–468, 1964.

Dee, D. P., Uppala, S. M., Simmons, A. J., Berrisford, P., Poli, P., Kobayashi, S., Andrae, U., Balmaseda, M. A., Balsamo, G., Bauer, P., Bechtold, P., Beljaars, A. C. M., van de Berg, L., Bidlot, J., Bormann, N., Delsol, C., Dragani, R., Fuentes, M., Geer, A. J., Haimberger, L., Healy, S. B., Hersbach, H., Hólm, E. V., Isaksen, L., Kållberg, P., Köhler, M., Matricardi, M., McNally, A. P., Monge-Sanz, B. M., Morcrette, J.-J., Park, B.-K., Peubey, C., de Rosnay, P., Tavolato, C., Thépaut, J.-N., and Vitart, F.: The ERA-Interim reanalysis: configuration and performance of the data assimilation system, Q. J. Roy. Meteor. Soc., 137, 553–597, doi:10.1002/qj.828, 2011.

Field, R. D.: Observed and modeled controls on precipitation delta ^{18}O over Europe: from local temperature to the Northern Annular Mode, J. Geophys. Res., 115, D12101, doi:10.1029/2009jd013370, 2010.

Frankenberg, C., Wunch, D., Toon, G., Risi, C., Scheepmaker, R., Lee, J.-E., Wennberg, P., and Worden, J.: Water vapor isotopologue retrievals from high-resolution GOSAT shortwave infrared spectra, Atmos. Meas. Tech., 6, 263–274, doi:10.5194/amt-6-263-2013, 2013.

Giorgetta, M., Jungclaus, J., Reick, C., Legutke, S., Brovkin, V., Crueger, T., Esch, M., Fieg, K., Glushak, K., Gayler, V., Haak, H., Hollweg, H.-D., Kinne, S., Kornblueh, L., Matei, D., Mauritsen, T., Mikolajewicz, U., Müller, W., Notz, D., Raddatz, T., Rast, S., Roeckner, E., Salzmann, M., Schmidt, H., Schnur, R., Segschneider, J., Six, K., Stockhause, M., Wegner, J., Widmann, H., Wieners, K.-H., Claussen, M., Marotzke, J., and Stevens, B.: CMIP5 simulations of the Max Planck Institute for Meteorology (MPI-M) based on the MPI-ESM-LR model: the rcp45 experiment, served by ESGF, doi:10.1594/WDCC/CMIP5.MXELr4, 2012.

Gribanov, K., Jouzel, J., Bastrikov, V., Bonne, J.-L., Breon, F.-M., Butzin, M., Cattani, O., Masson-Delmotte, V., Rokotyan, N., Werner, M., and Zakharov, V.: ECHAM5-wiso water vapour isotopologues simulation and its comparison with WS-CRDS measurements and retrievals from GOSAT and ground-based FTIR spectra in the atmosphere of Western Siberia, Atmos. Chem. Phys. Discuss., 13, 2599–2640, doi:10.5194/acpd-13-2599-2013, 2013.

Gryazin, V., Risi, C., Jouzel, J., Kurita, N., Worden, J., Frankenberg, C., and Bastrikov, V.: Added value of water isotopic measurements to understand model biases in simulated water cycle in western Siberia, Atmos. Chem. Phys. Discuss., in preparation, 2013.

Haese, B., Werner, M., and Lohmann, G.: Stable water isotopes in the coupled atmosphere–land surface model ECHAM5-JSBACH, Geosci. Model Dev., 6, 1463–1480, doi:10.5194/gmd-6-1463-2013, 2013.

Hagemann, S., Arpe, K., and Roeckner, E.: Evaluation of the hydrological cycle in the ECHAM5 model, J. Climate, 19, 3810–3827, doi:10.1175/JCLI3831.1, 2006.

Halpert, M. S. and Bell, G. D.: Climate Assessment for 1996, B. Am. Meteorol. Soc., 78, 1038, doi:10.1175/1520-0477(1997)078<1038:CAF>2.0.CO;2, 1997.

Hoffmann, G., Werner, M., and Heimann, M.: Water isotope module of the ECHAM atmospheric general circulation model: a study on timescales from days to several years, J. Geophys. Res., 103, 16871–16896, 1998.

Holland, M. M. and Bitz, C. M.: Polar amplification of climate change in coupled models, Clim. Dynam., 21, 221–232, doi:10.1007/s00382-003-0332-6, 2003.

ACPD
13, 29263–29301, 2013

Hurrell, J. and National Center for Atmospheric Research Staff (Eds.): The Climate Data Guide: Hurrell North Atlantic Oscillation (NAO) Index (station-based), retrieved from https://climatedataguide.ucar.edu/climate-data/hurrell-north-atlantic-oscillation-nao-index-station-based (last access: 16 September 2013), 2013.

Hurrell, J. W. and Deser, C.: North Atlantic climate variability: the role of the North Atlantic Oscillation, J. Mar. Syst., 78, 28–41, doi:10.1016/j.jmarsys.2008.11.026, 2009.

IAEA/WMO: Global Network of Isotopes in Precipitation. The GNIP Database, accessible at: http://www.iaea.org/water (last access: 2 July 2013), 2013.

IPCC: Contribution of Working Group I to the Fourth Assessment Report of the Intergovernmental Panel on Climate Change, Cambridge University Press, Cambridge, UK and New York, NY, USA, 2007.

Joussaume, S., Sadourny, R., and Jouzel, J.: A general circulation model of water isotope cycles in the atmosphere, Nature, 311, 24–29, doi:10.1038/311024a0, 1984.

Jouzel, J. and Merlivat, L.: Deuterium and oxygen 18 in precipitation: modeling of the isotopic effects during snow formation, J. Geophys. Res., 89, 11749–11757, doi:10.1029/JD089iD07p11749, 1984.

Jouzel, J., Russell, G. L., Suozzo, R. J., Koster, R. D., White, J. W. C., and Broecker, W. S.: Simulations of the HDO and $H_2^{18}O$ atmospheric cycles using the NASA GISS General Circulation Model: the seasonal cycle for present-day conditions, J. Geophys. Res., 92, 14739–14760, doi:10.1029/JD092iD12p14739, 1987.

Jouzel, J., Hoffmann, G., Koster, R. D., and Masson, V.: Water isotopes in precipitation: data/model comparison for present-day and past climates, Quat. Sci. Rev., 19, 363–379, 2000.

Koster, R. D., de Valpine, D. P., and Jouzel, J.: Continental water recycling and $H_2^{18}O$ concentrations, Geophys. Res. Lett., 20, 2215–2218, 1993.

Krishnamurti, T. N., Xue, J., Bedi, H. S., Ingles, K., Oosterhof, D.: Physical initialization for numerical weather prediction over the tropics, Tellus A, 43, 53–81, 1991.

Kurita, N., Numaguti, A., Sugimoto, A., Ichiyanagi, K., and Yoshida, N.: Relationship between the variation of isotopic ratios and the source of summer precipitation in eastern Siberia, J. Geophys. Res., 108, 4339, doi:10.1029/2001JD001359, 2003.

Kurita, N., Yoshida, N., and Chayanova, E. A.: Modern isotope climatology of Russia: a first assessment, J. Geophys. Res., 109, D3102, doi:10.1029/2003JD003404, 2004.

ACPD
13, 29263–29301, 2013

Variations of oxygen-18 in west Siberian precipitation

M. Butzin et al.

Langebroek, P. M., Werner, M., and Lohmann, G.: Climate information imprinted in oxygen-isotopic composition of precipitation in Europe, Earth Planet. Sci. Lett., 311, 144–154, doi:10.1016/j.epsl.2011.08.049, 2011.

Lee, J. E. and Fung, I.: "Amount effect" of water isotopes and quantitative analysis of post-condensation processes, Hydrol. Process., 22, 1–8, doi:10.1002/Hyp.6637, 2008.

Lin, S.-J. and Rood, R. B.: Multidimensional flux-form semi Lagrangian transport schemes, Mon. Weather Rev., 124, 2046–2070, doi:10.1175/1520-0493(1996)124<2046:MFFSLT>2.0.CO;2, 1996.

Mathieu, R., Pollard, D., Cole, J. E., White, J. W. C., Webb, R. S., and Thompson, S. L.: Simulation of stable water isotope variations by the GENESIS GCM for modern conditions, J. Geophys. Res.-Atmos., 107, 4037, doi:10.1029/2001JD900255, 2002.

Merlivat, L. and Jouzel, J.: Global climatic interpretation of the deuterium-oxygen 18 relationship for precipitation, J. Geophys. Res., 84, 5029–5033, 1979.

Merlivat, L., Ravoire, J., Vergnaud, J. P., and Lorius, C.: Tritium and deuterium content of snow in Greenland, Earth Planet. Sci. Lett., 19, 235–240, 1973.

Noone, D. and Simmonds, I.: Associations between δ^{18}O of water and climate parameters in a simulation of atmospheric circulation for 1979–95, J. Climate, 15, 3150–3169, 2002.

Numaguti, A.: Origin and recycling processes of precipitating water over the Eurasian continent: experiments using an atmospheric general circulation model, J. Geophys. Res., 104, 1957–1972, doi:10.1029/1998JD200026, 1999.

Polyakov, I. V., Alekseev, G. V., Bekryaev, R. V., Bhatt, U., Colony, R. L., Johnson, M. A., Karklin, V. P., Makshtas, A. P., Walsh, D., and Yulin, A. V.: Observationally based assessment of polar amplification of global warming, Geophys. Res. Lett., 29, 1878, doi:10.1029/2001GL011111, 2002.

Rast, S., Brokopf, R., Cheedela, S.-K., Esch, M., Gayler, Kirchner, I., Kornblüh, L., Rhodin, A., Schmidt, H., Schulzweida, U., Wieners, K.-H.: User Manual for ECHAM6, Reports on Earth System Science 13, Max Planck Institute for Meteorology, Hamburg, Germany, 2013.

Risi, C., Bony, S., Vimeux, F., and Jouzel, J.: Water-stable isotopes in the LMDZ4 general circulation model: model evaluation for present-day and past climates and applications to climatic interpretations of tropical isotopic records, J. Geophys. Res., 115, D12118, doi:10.1029/2009JD013255, 2010a.

Risi, C., Bony, S., Vimeux, F., Frankenberg, C., Noone, D., and Worden, J.: Understanding the Sahelian water budget through the isotopic composition of water vapor and precipitation, J. Geophys. Res., 115, D24110, doi:10.1029/2010JD014690, 2010b.

Risi, C., Noone, D., Frankenberg, C., and Worden, J.: Role of continental recycling in intraseasonal variations of continental moisture as deduced from model simulations and water vapor isotopic measurements, Water Resour. Res., 49, 1–21, doi:10.1002/wrcr.20312, 2013.

Roeckner, E., Bäuml, G., Bonaventura, L. Brokopf, R., Esch, M., Giorgetta, M., Hagemann, S., Kirchner, I., Kornblueh, L., Manzini, E., Rhodin, A., Schlese, U., Schulzweida, U., and Tompkins, A.: The atmospheric general circulation model ECHAM5, Part 1, Model description, Report No. 349, Max Planck Institute for Meteorology, Hamburg, Germany, 2003.

Roeckner, E., Brokopf, R., Esch, M., Giorgetta, M., Hagemann, S., Kornblueh, L., Manzini, E.,Schlese, U., and Schulzweida, U.: Sensitivity of simulated climate to horizontal and vertical resolution in the ECHAM5 atmosphere model, J. Climate, 19, 3771–3791, doi:10.1175/JCLI3824.1, 2006.

Rokotyan, N. V, Zakharov, V. I., Gribanov, K. G, Bréon, F- M., Jouzel, J., Imasu, R., Werner, M., Butzin, M, Petri, C., Warneke, T., Notholt, J.: Retrieval of δ^{18}O and δD in the atmospheric water vapour from high-resolution ground-based FTIR measurements of solar radiation in near-infrared, Atmos. Meas. Tech. Discuss., submitted, 2013.

Saurer, M., Schweingruber, F., Vaganov, E. A., Shiyatov, S. G., and Siegwolf, R.: Spatial and temporal oxygen isotope trends at the northern tree-line in Eurasia, Geophys. Res. Lett., 29, 1296, doi:10.1029/2001GL013739, 2002.

Schmidt, G. A., Hoffmann, G., Shindell, D. T., and Hu, Y.: Modeling atmospheric stable water isotopes and the potential for constraining cloud processes and stratosphere-troposphere water exchange, J. Geophys. Res., 110, D21314, doi:10.1029/2005JD005790, 2005.

Screen, J. A. and Simmonds, I.: The central role of diminishing sea ice in recent Arctic temperature amplification, Nature, 464, 1334–1337, doi:10.1038/nature09051, 2000.

Serreze, M. and Francis, J.: The Arctic Amplification Debate, Clim. Change, 76, 241–264, doi:10.1007/s10584-005-9017-y, 2006.

Sidorova, O. V., Siegwolf, R. T. W., Saurer, M., Naurzbaev, M. M., Shashkin, A. V., and Vaganov, E. A.: Spatial patterns of climatic changes in the Eurasian north reflected in Siberian larch tree-ring parameters and stable isotopes, Glob. Change Biol., 16, 1003–1018, 2010.

ACPD
13, 29263–29301, 2013

Variations of oxygen-18 in west Siberian precipitation

M. Butzin et al.

Sonntag, C., Neureuther, P., Kalinke, C., Münnich, K. O., Klitzsch, E., and Weistroffer, K.: Zur Paläoklimatik der Sahara, Naturwissenschaften, 63, 479–479, doi:10.1007/BF00624580, 1976.

Sturm, C., Zhang, Q., and Noone, D.: An introduction to stable water isotopes in climate models: benefits of forward proxy modelling for paleoclimatology, Clim. Past, 6, 115–129, doi:10.5194/cp-6-115-2010, 2010.

Taylor, P. C., Cai, M., Hu, A., Meehl, J., Washington, W., and Zhang, G. J.: A decomposition of feedback contributions to polar warming amplification, J. Climate, 26, 7023–7043, 2013.

Tindall, J. C., Valdes, P. J., and Sime, L. C.: Stable water isotopes in HadCM3: isotopic signature of El Niño–Southern Oscillation and the tropical amount effect, J. Geophys. Res., 114, D04111, doi:10.1029/2008JD010825, 2009.

Tingley, M. P. and Huybers, P.: Recent temperature extremes at high northern latitudes unprecedented in the past 600 years, Nature, 496, 201–208, doi:10.1038/nature11969, 2013.

Trenberth, K. E., Jones, P. D., Ambenje, P., Bojariu, R., Easterling, D., Klein Tank, A., Parker, D., Rahimzadeh, F., Renwick, J. A., Rusticucci, M., Soden, B., and Zhai, P.: Observations: surface and atmospheric climate change, in: Climate Change 2007: The Physical Science Basis. Contribution of Working Group I to the Fourth Assessment Report of the Intergovernmental Panel on Climate Change, edited by: Solomon, S., Qin, D., Manning, M., Chen, Z., Marquis, M., Averyt, K. B., Tignor, M., and Miller, H. L., Cambridge University Press, Cambridge, UK and New York, NY, USA, 2007.

University of East Anglia Climatic Research Unit (CRU), Jones, P. and Harris, I.: CRU TS3.21: Climatic Research Unit (CRU) Time-Series (TS) Version 3.21 of High Resolution Gridded Data of Month-by-month Variation in Climate (January 1901–December 2012), [Internet], NCAS British Atmospheric Data Centre, available from: http://badc.nerc.ac.uk/view/badc.nerc.ac.uk__ATOM__ACTIVITY_0c08abfc-f2d5-11e2-a948-00163e251233, doi:10.5285/D0E1585D-3417-485F-87AE-4FCECF10A992 (last access: 18 September 2013), 2013.

Uppala, S. M., Kållberg, P. W., Simmons, A. J., Andrae, U., da Costa Bechtold, V., Fiorino, M., Gibson, J. K., Haseler, J., Hernandez, A., Kelly, G. A., Li, X., Onogi, K., Saarinen, S., Sokka, N., Allan, R. P., Andersson, E., Arpe, K., Balmaseda, M. A., Beljaars, A. C. M., van de Berg, L., Bidlot, J., Bormann, N., Caires, S., Chevallier, F., Dethof, A., Dragosavac, M., Fisher, M., Fuentes, M., Hagemann, S., Hólm, E., Hoskins, B. J., Isaksen, L., Janssen, P. A. E. M., Jenne, R., McNally, A. P., Mahfouf, J.-F., Morcrette, J.-J.,

ACPD
13, 29263–29301, 2013

Rayner, N. A., Saunders, R. W., Simon, P., Sterl, A., Trenberth, K. E., Untch, A., Vasiljevic, D., Viterbo, P., and Woollen, J.: The ERA-40 re-analysis, Q. J. Roy. Meteor. Soc., 131, 2961–3012, doi:10.1256/qj.04.176, 2005.
Vuille, M. and Werner, M.: Stable isotopes in precipitation recording South American summer monsoon and ENSO variability: observations and model results, Clim. Dynam., 25, 401–413, 2005.
Werner, M. and Heimann, M.: Modeling interannual variability of water isotopes in Greenland and Antarctica, J. Geophys. Res., 107, 4001, doi:10.1029/2001JD900253, 2002.
Werner, M., Heimann, M., and Hoffmann, G.: Isotopic composition and origin of polar precipitation in present and glacial climate simulations, Tellus B, 53, 53–71, doi:10.1034/j.1600-0889.2001.01154.x, 2001.
Werner, M., Langebroek, P. M., Carlsen, T., Herold, M., and Lohmann, G.: Stable water isotopes in the ECHAM5 general circulation model: toward high-resolution isotope modeling on a global scale, J. Geophys. Res., 116, D15109, doi:10.1029/2011jd015681, 2011.
Yoshimura, K., Frankenberg, C., Lee, J., Kanamitsu, M., Worden, J., and Röckmann, T.: Comparison of an isotopic atmospheric general circulation model with new quasi-global satellite measurements of water vapor isotopologues, J. Geophys. Res., 116, D19118, doi:10.1029/2011JD016035, 2011.

Table 1. GNIP δ^{18}O records from Russia considered in this study.

Name	Lat (° N)	Lon (° E)	Alt (m)	t_{obs} δ^{18}O	$N_{obs}\delta^{18}$O
Arkhangelsk	64.58	40.50	13	1981–1990	78
Astrakhan	46.25	48.03	−18	1980–2000	168
Bagdarin	54.47	113.58	903	1996–2000	34
Barabinsk	**55.33**	**78.37**	**120**	**1996–2000**	**37**
Cherskiy	68.76	161.34	30	2001–2009	57
Kalinin	56.90	35.90	31	1980–1988	94
Kirov	58.65	49.62	164	1980–2000	102
Moscow	55.75	37.57	157	1970–1979	61
Murmansk	68.97	33.05	46	1980–1990	71
Pechora	**61.12**	**57.10**	**56**	**1980–1990**	**79**
Perm	**57.95**	**56.20**	**161**	**1980–1990**	**79**
Rostov	47.25	39.82	77	1980–1990	74
Saratov	51.57	46.03	166	1980–1990	74
St. Petersburg	59.97	30.30	4	1980–1990	107
Yakutsk	62.08	129.75	107	1978–2000	46

Stations located in western Siberia are highlighted in bold. For each station, we report the latitude, longitude and altitude, as well as the sampling period (t_{obs}) and the number of available monthly measurements (N_{obs}).

ACPD
13, 29263–29301, 2013

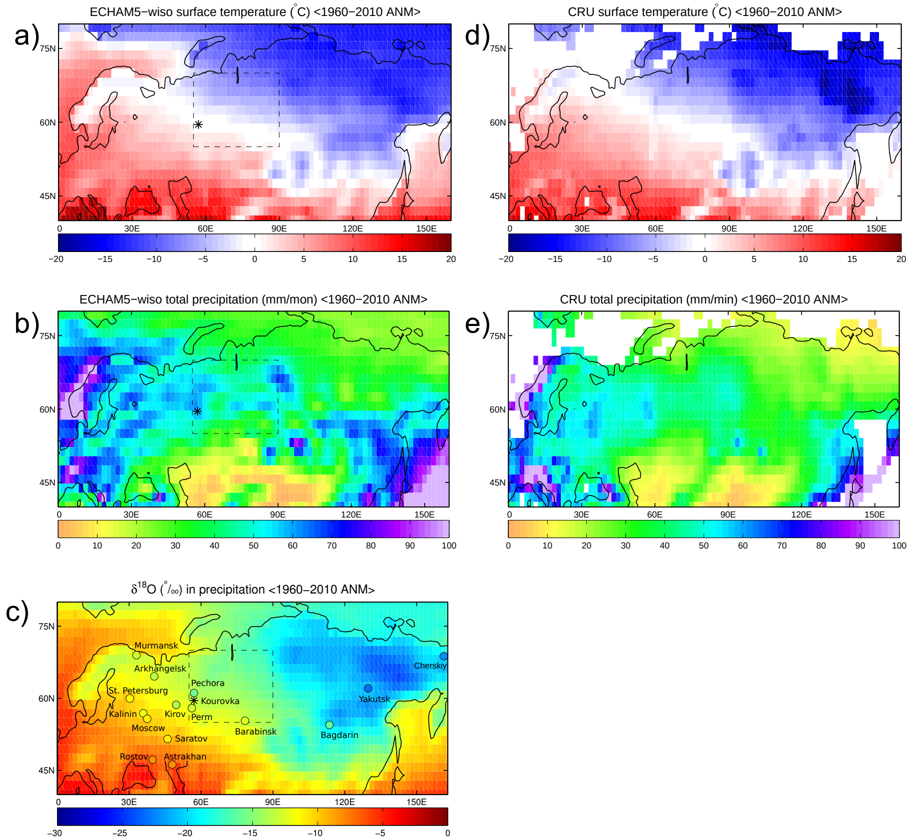

Fig. 1. Left column: Simulated mean annual values of **(a)** surface temperature, **(b)** precipitation, and **(c)** $\delta^{18}O$ in precipitation, averaged over the period 1960–2010. Right column: CRU data of **(d)** surface temperature, and **(e)** precipitation amount, averaged over the same period. The circles in **(c)** mark the position of the various GNIP stations used for analyses in this study.

ACPD
13, 29263–29301, 2013

Variations of oxygen-18 in west Siberian precipitation

M. Butzin et al.

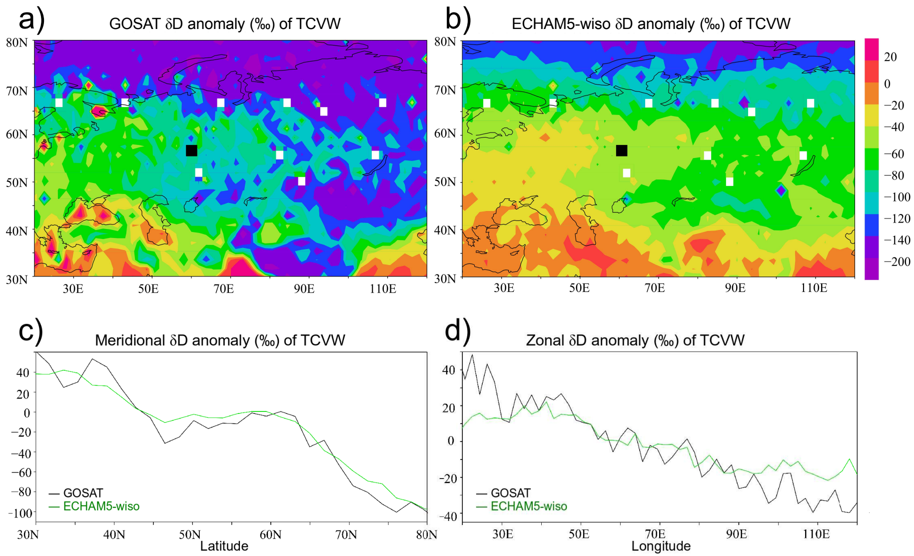

Fig. 2. Distribution of annual-mean δD in total column water vapour, **(a)** as observed by the GOSAT satellite, **(b)** as simulated by ECHAM, after collocation with GOSAT observations and convolution with the corresponding averaging kernels. In **(a)** and **(b)** the global average of δD has been subtracted to highlight spatial patterns, and the black squares indicate the location of Kourovka Observatory. **(c)** Meridional transects of observed (black) and simulated (green) δD averaged over the longitude band 50–70° E around Kourovka. The annual-mean δD value averaged over the area 30–80° N, 50–70° E has been subtracted to highlight the meridional variations. **(d)** Zonal transects of observed (black) and simulated (green) δD averaged over the latitude band 50–64° N around Kourovka. The annual-mean δD value averaged over the area 50–64° N, 20–120° E has been subtracted to highlight the zonal variations.

ACPD
13, 29263–29301, 2013

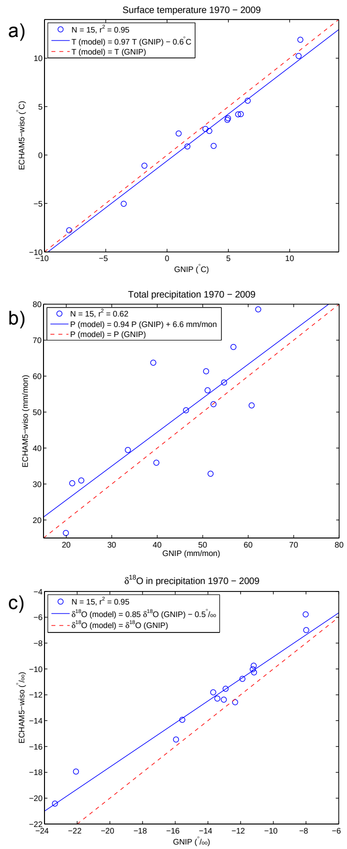

Fig. 3. Comparison of mean values of **(a)** surface temperature, **(b)** precipitation amount, and **(c)** δ^{18}O in precipitation for a selection of 15 GNIP stations located in Russia and the related ECHAM5-wiso model results. (See text for details on station selection and mean value calculation at each station.)

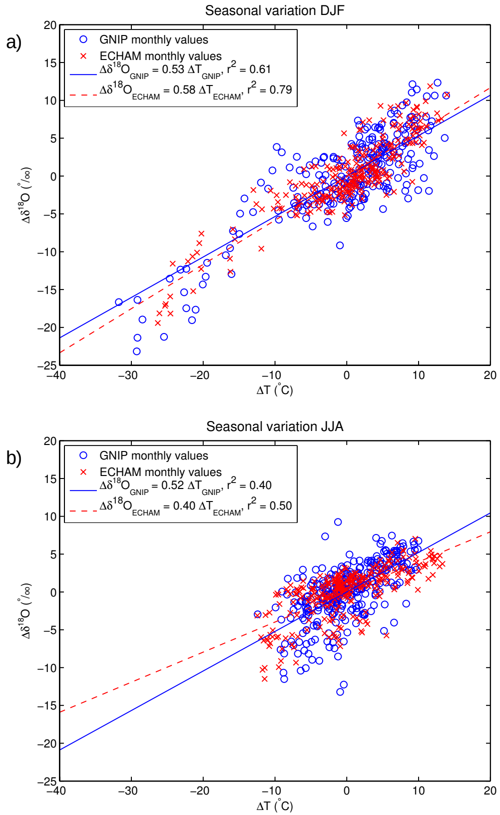

Fig. 4. Relationship between $\delta^{18}O$ and surface temperature. Shown are monthly anomalies ($\Delta\delta^{18}O$ and ΔT) according to monthly observations from 15 GNIP stations in Russia (circles) and the related ECHAM5-wiso model results (crosses), **(a)** winter season, **(b)** summer season. Also shown are linear regression lines for observations (solid lines) and model results (dashed lines).

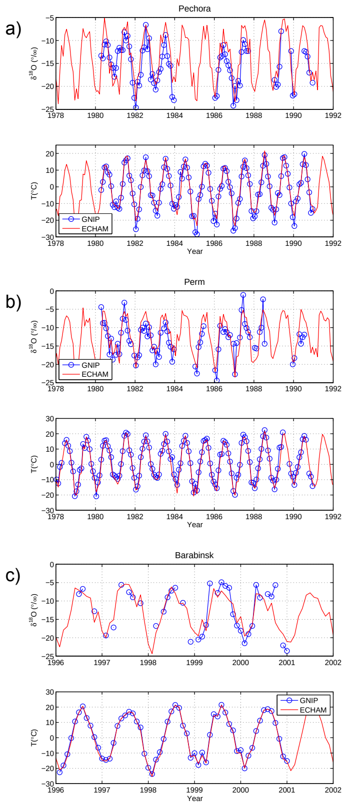

Fig. 5. Observed vs. modelled monthly $\delta^{18}O$ values in precipitation for the period 1980–2000. Measurements of 3 GNIP stations located in western Siberia are plotted as blue circles: **(a)** Pechora, **(b)** Perm, **(c)** Barabinsk. The red line shows ECHAM5-wiso results corresponding to the same locations. Also shown are observed (blue) and modelled (red) surface temperatures.

ACPD
13, 29263–29301, 2013

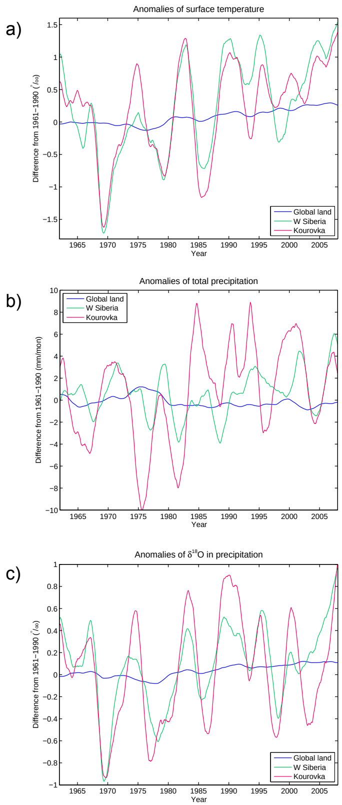

Fig. 6. Simulated time series of **(a)** surface temperature, **(b)** precipitation, and **(c)** $\delta^{18}O$ in precipitation for the period 1962–2008. Shown are anomalies from the climatological mean (reference period: 1961–1990). The ECHAM5-wiso results are averaged globally (blue line), for the region of western Siberia (green line), and interpolated to the location of Kourovka Observatory (red line). A zero-phase bidirectional low-pass filter with a length of 24 equally weighted months has been applied to the simulated monthly mean values for filtering short-term fluctuations.

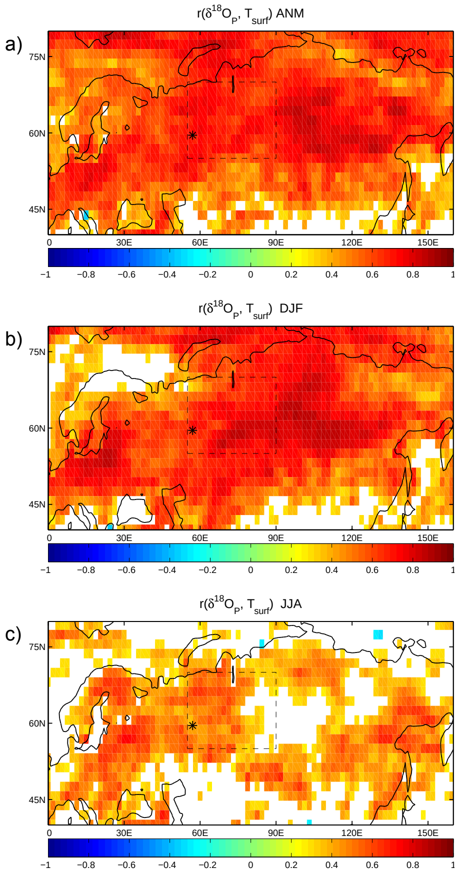

Fig. 7. Temporal correlation between simulated values of δ^{18}O in precipitation and surface temperatures for the period 1960–2010. Correlation coefficients are calculated for **(a)** annual mean, **(b)** winter (DJF), and **(c)** summer (JJA) values of temperature and δ^{18}O.

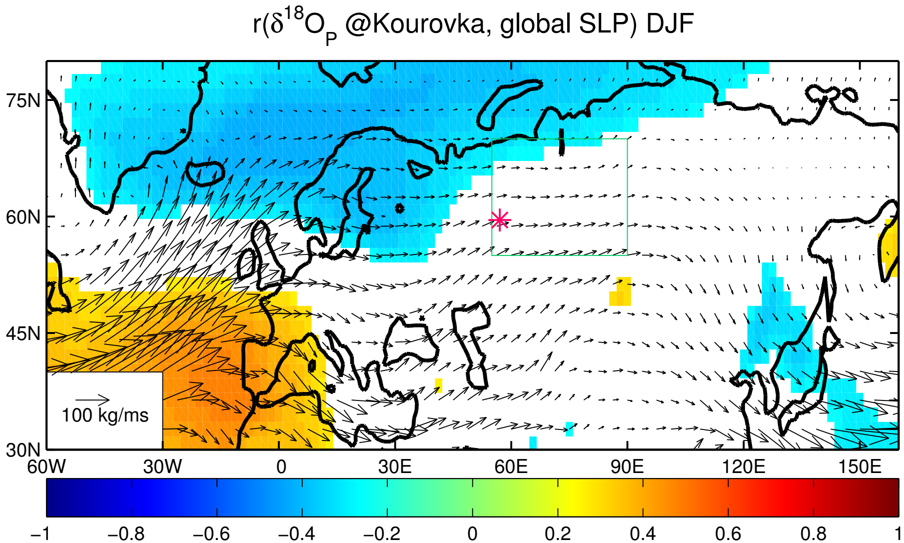

Fig. 8. One-point correlation map showing the correlation between global sea-level pressure and δ^{18}O in precipitation at Kourovka during the winter season (DJF, correlation period is 1960–2010). Also shown is the average atmospheric moisture transport during DJF (vectors; only every second vector is drawn). The green box indicates western Siberia, position of Kourovka is marked by a red star.

ACPD
13, 29263–29301, 2013

Variations of oxygen-18 in west Siberian precipitation

M. Butzin et al.

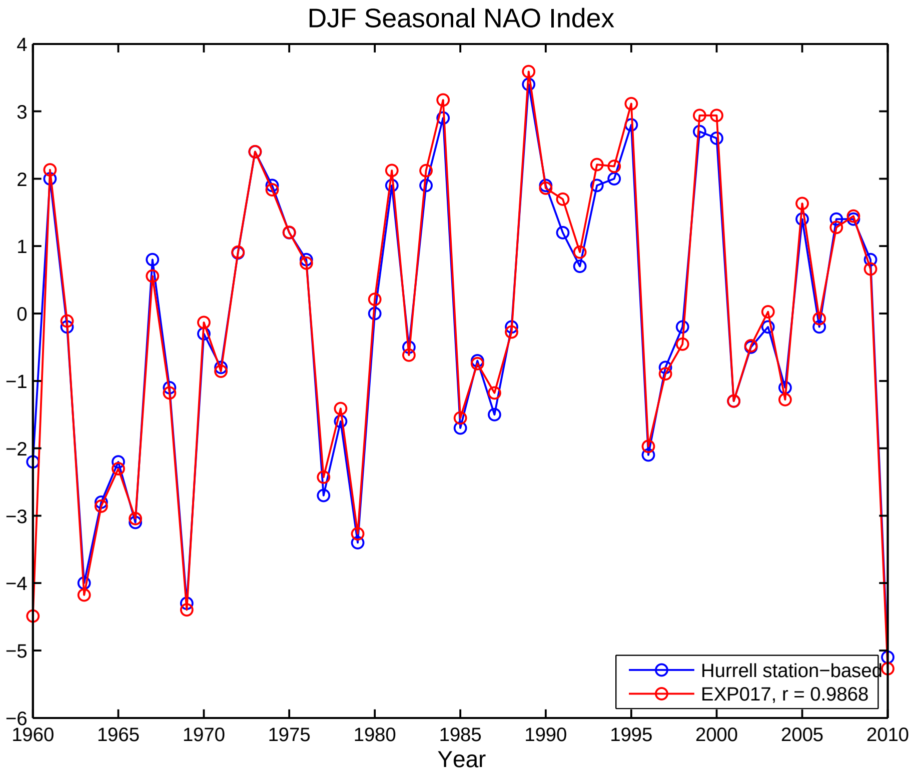

Fig. 9. NAO winter (DJF) station index for the period 1960–2010, according to observations (blue line; Hurrell et al., 2013), and as simulated by the ECHAM5-wiso model (red line).

ACPD
13, 29263–29301, 2013

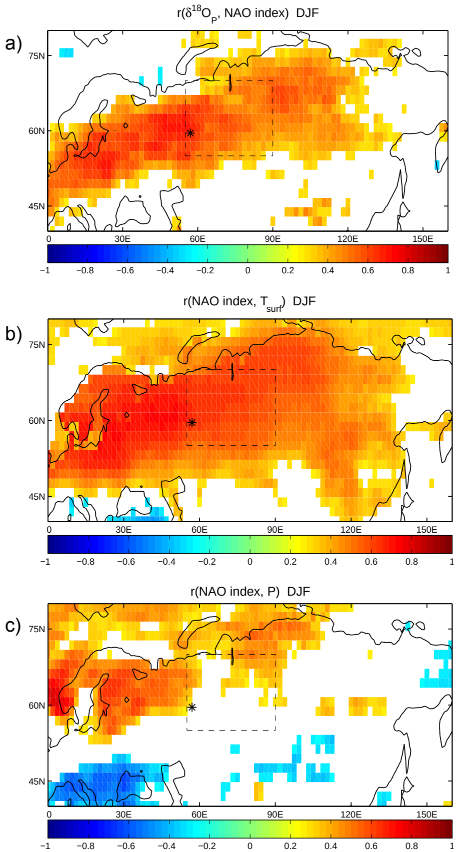

Fig. 10. Temporal correlation between station-based NAO winter (DJF) index and **(a)** $\delta^{18}O$ in precipitation, **(b)** surface temperature, and **(c)** total precipitation amount. Statistically insignificant areas (where $p \geq 0.05$ applying a t test) are blanked.

ACPD
13, 29263–29301, 2013

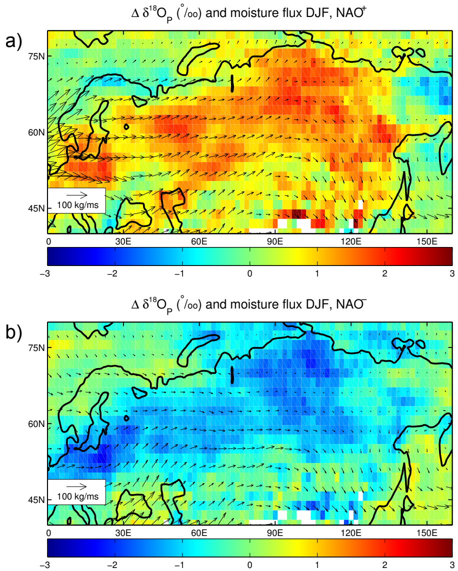

Fig. 11. Simulated moisture transport (vectors; only every second vector is drawn) and anomalies of $\delta^{18}O$ in precipitation (colours) for **(a)** average strong NAO$^+$, and **(b)** weak NAO$^-$ conditions.

Discussion Paper | Discussion Paper | Discussion Paper | Discussion Paper |

ACPD

13, 29263–29301, 2013

Variations of oxygen-18 in west Siberian precipitation

M. Butzin et al.

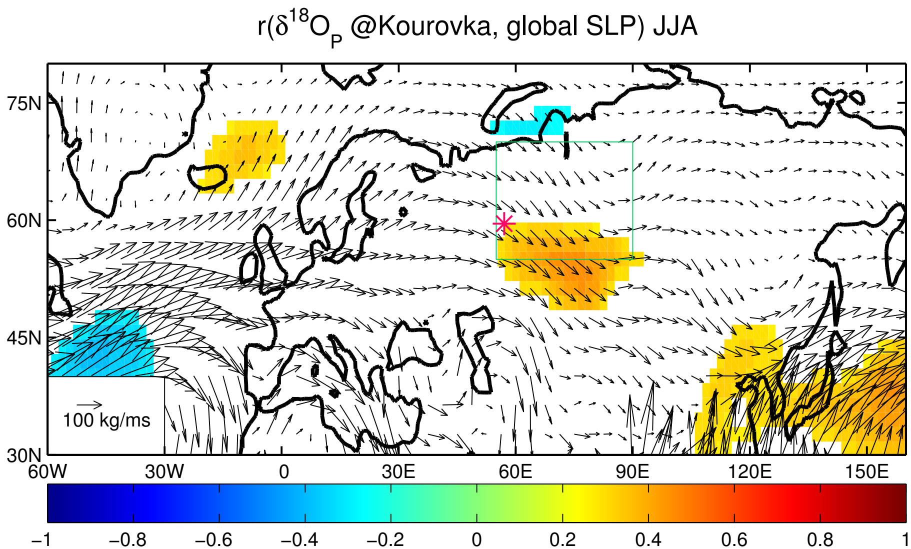

Fig. 12. One-point correlation map showing the correlation between global sea-level pressure and δ^{18}O in precipitation at Kourovka during the summer season (JJA, correlation period is 1960–2010). Also shown is the average atmospheric moisture transport during JJA (vectors; only every second vector is drawn). The green box indicates western Siberia, position of Kourovka is marked by a red star.

ACPD
13, 29263–29301, 2013